


Article

The Synthesis and Pharmacokinetics of a Novel Liver-Targeting Cholic Acid-Conjugated Carboplatin in Rats

Yinyin Lan ^{1,2,†}, Fuguo Han ^{2,†}, Anli Gao ^{3,†}, Xuemei Fan ², Yanli Hao ², Zhao Wang ², Weiping Liu ³, Jing Jiang ^{3,*} and Qingfei Liu ^{2,*} 

¹ School of Pharmacy, Shaanxi University of Chinese Medicine, Xianyang 712046, China; lyy754869196@163.com

² School of Pharmaceutical Sciences, Tsinghua University, Beijing 100084, China; hanfg2001@tsinghua.edu.cn (F.H.); xuemeifan@tsinghua.edu.cn (X.F.); haoyanli@tsinghua.edu.cn (Y.H.); tcm@tsinghua.edu.cn (Z.W.)

³ Kunming Institute of Precious Metals, Kunming 650106, China; gaoanli@126.com (A.G.); liuweiping0917@126.com (W.L.)

* Correspondence: jiangjing_85@126.com (J.J.); liuqf@tsinghua.edu.cn (Q.L.)

† These authors contributed equally to this work.

Abstract: A novel cholic acid-conjugated carboplatin (CP-CA) is developed as a liver-targeting prodrug of carboplatin (CP) for liver cancer. Instead of using CP as a raw material, CP-CA was synthesized simultaneously. This paper is focused on the comparison of CP-CA and CP with respect to their pharmacokinetic (PK) and tissue distribution profiles in rats after their intravenous administration. Additionally, their uptake by human liver tumor cell Huh7 and normal human liver cell HL7702 are investigated. The inductively coupled plasma mass spectrometry (ICP-MS) method is applied for the determination of platinum in plasma, tissues, and cells. The PK results show that both the AUC_{0-t} and $AUC_{0-\infty}$ data on Pt for CP-CA are significantly higher than those for CP ($p < 0.01$), indicating that the plasma exposure of CP-CA is significantly higher than that of CP. The CL_1 , Vd_1 , and Vd_2 data on Pt for CP-CA are significantly lower than those for CP ($p < 0.01$), while the MRT_{0-t} is significantly higher ($p < 0.01$), which is possibly related to a higher PPBR, and can strongly support the higher AUC_{0-t} and $AUC_{0-\infty}$ of Pt for CP-CA compared to for CP. The tissue distribution results show that CP-CA is mainly distributed and accumulated in the liver after its intravenous administration to rats, revealing its liver-targeting profile. Compared to CP, CP-CA is more easily taken up by human liver cancer cells and normal human liver cells. The results suggest that CP-CA has a potential for further development as a new prodrug specific to liver cancer.

Keywords: carboplatin; cholic acid conjugation; pharmacokinetics; tissue distribution; liver cancer



Citation: Lan, Y.; Han, F.; Gao, A.; Fan, X.; Hao, Y.; Wang, Z.; Liu, W.; Jiang, J.; Liu, Q. The Synthesis and Pharmacokinetics of a Novel Liver-Targeting Cholic Acid-Conjugated Carboplatin in Rats. *Inorganics* **2024**, *12*, 184. <https://doi.org/10.3390/inorganics12070184>

Academic Editor: Isabel Correia

Received: 6 May 2024

Revised: 1 June 2024

Accepted: 12 June 2024

Published: 30 June 2024



Copyright: © 2024 by the authors. Licensee MDPI, Basel, Switzerland. This article is an open access article distributed under the terms and conditions of the Creative Commons Attribution (CC BY) license (<https://creativecommons.org/licenses/by/4.0/>).

1. Introduction

Currently, cancer is still a global and urgent problem and it seriously threatens human health and life quality [1]. Taking China as an example, approximately 410,000 patients were newly diagnosed with liver cancer in 2020, accounting for 45.3% of new cases globally [2]. Chemotherapy together with surgical operation, radiotherapy, or biotherapy is the main approach to cancer treatment. However, the biggest characteristic of chemotherapy is its inability to distinguish between cancer cells and normal cells, resulting in significant toxicity and side effects. Over the past two decades, there has been a tremendous shift in cancer treatment from broad-spectrum cytotoxic drugs to targeted drugs [3]. Targeted therapy has undoubtedly become a key and urgent area of anticancer drug research due to its advantages, such as delivering therapeutic agents directly to tumor sites while minimizing drug-related toxicities, which can significantly improve chemotherapeutic efficiency.

Platinum (Pt)-based drugs, exemplified by cisplatin (CIS), carboplatin (CP), and oxaliplatin (OXA), have become the first-line cytotoxic treatment of various kinds of human

cancer such as ovarian, lung, and prostate cancer, and they work by interacting with the DNA of cancer cells, leading to the disruption of normal cell functions and ultimately cell death. However, like many other traditional chemotherapy reagents, Pt-based drugs also have severe toxicities and side effects due to their poor active selection, which has limited their clinical application [4]. CP, for instance, has become a second-generation Pt-based drug, but CP-related hypersensitivity reactions (HSRs) may occur within minutes or even hours after infusion, characterized by the development of mild symptoms, such as erythema, pruritus, and urticaria, as well as severe symptoms, including difficulties in breathing, hypotension, anaphylaxis, cardiovascular collapse, and even death [5–7]. It is therefore rational to choose carboplatin, with its target area under the curve (AUC), as an element of pretreatment or concomitantly administered chemotherapies, supported by clinical pharmacokinetics [8]. In order to improve the targeting effect of Pt-based drugs, two main strategies have been developed in recent years: one is using nanocarriers to deliver drugs, including carbon nanotubes, carbon nanoparticles, gold nanoparticles, quantum dots, upconversion nanoparticles, and polymeric micelles, and the other one is modifying the drug with different functional groups, such as glucose and PEGylated folate [9–12].

It has been recognized that liver epithelial cells express certain transport proteins responsible for the uptake of bile salts from the bloodstream [13]. Therefore, it is a logical deduction that bile acids, such as cholic acid, chenodeoxycholic acid, ursodeoxycholic acid, etc., can serve as vectors to deliver therapeutic agents to the liver, which has been firmly supported by many cases [14–17]. For instance, cholic acid-conjugated fluorouracil and cytarabine both showed liver specificity, with a significant increase in drug concentration in the liver tissue [18,19], and ursodeoxycholic acid-modified cisplatin could be taken up through the natural uptake pathway utilized by bile acids, leading to its enhanced cytostatic activity against liver tumors [20]. In addition, several bile acid receptors such as FXR, GPBAR, SLC10A1, TGR5, and NTCP have been identified and showed great potential as drug targets for anticancer drug development. Drugs can be modified with bile acids or their derivatives to target liver cancer cells via the transport systems of bile acids [21–23]. For example, three cholic acid-conjugated cytarabines had better liver-targeting effects and higher absorption compared to cytarabine [24]. A series of Pt complexes conjugated with other bile acids such as cholyglycinate, ursodeoxycholate, and bis ursodeoxycholate also showed synergistic effects in their anticancer activities [25–27]. For instance, platinum(II) bile acid derivatives, named Bamets, could affect the ability of these compounds to interact with DNA and reduce tumor cell growth. The distance between the platinum atom and the bile acid moiety affects the Bamet's *in vitro* reactivity with DNA [28,29]. The amount of Bamets, but not cisplatin, taken up by XO was enhanced when they expressed OATP-A, OATP-C, NTCP, OCT1, or OCT2, and a non-hepatic OCT isoform was used for comparative purposes [30].

Recently, we reported a novel prodrug of oxaliplatin named LLC-202, which was a cholic acid-conjugated oxaliplatin and was developed for liver cancer. It was synthesized using 3-NH₂-cyclobutane-1,1-dicarboxylate as a linker between its oxaliplatin analog and cholic acid moiety. It was mainly distributed and accumulated in the liver after its intravenous administration to rats, revealing its liver-targeting profile. It exhibited higher *in vitro* anticancer activity and an efficacy comparable to that of oxaliplatin in treating primary hepatocellular carcinoma in C57BL/6 mice [31]. With a similar strategy, we synthesized a cholic acid-conjugated carboplatin (CP-CA) (Figure 1), in which a cholic acid, as the liver-targeting moiety, is linked to CP at the position C₃ of 1,1-cyclobutane-dicarboxylic acid by an amide bond. Preliminary studies have shown its good *in vitro* and *in vivo* antitumor activity. The objective of this paper is to investigate the PK profiles and tissue distribution of CP-CA compared with its parent drug CP after their intravenous administration to rats. In addition, the uptake of CP-CA and CP by normal liver cells and liver tumor cells are also investigated and compared.

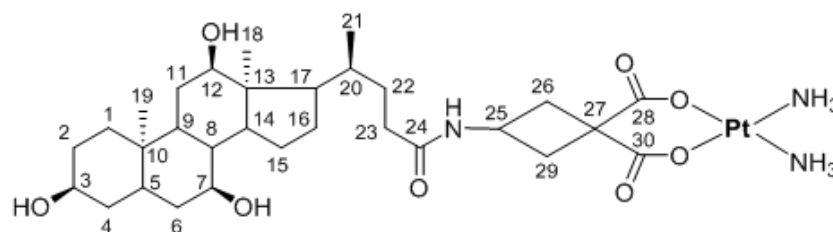


Figure 1. Chemical structure of cholic acid-conjugated carboplatin (CP-CA). The numbers 1 through 30 represent the sequential order of the carbon atoms in the molecular structure.

2. Results and Discussion

2.1. Structural Characterization of CP-CA

The structural characterization of CP-CA (Figure 1) was conducted through elemental composition analysis, HRESI⁺-MS, IR, as well as ¹H NMR, ¹³C-NMR, and 2D NMR spectra (Supplementary Materials). Calcd. % for C₃₀H₅₁N₃O₈Pt: C, 46.39; H, 6.57; N, 5.41; Pt, 25.13. Found: C, 46.10; H, 6.61; N, 5.36; Pt, 25.00. HRESI⁺-MS: [M + Na]⁺ m/z Calcd. = 799.3222 (¹⁹⁵Pt), Found = 799.3203. MS (ESI⁺) m/z, 799 ([M + Na]⁺); 777 ([M + H]⁺). IR (KBr, cm⁻¹): 3440 (s, ν_{O-H}), 3210 (s, ν_{N-H}), 1633 (vs, ν_{as}(COO)), 1378 (s, ν_a(COO)), 582 (w, ν_{Pt-N}), 492 (w, ν_{Pt-O}). ¹H NMR (500 MHz, DMSO-*d*₆) δ 8.09–7.76 (m, 1H, CONH), 4.32 (s, 2H, H-OH, H-OH), 4.21–3.86 (m, 7H, H-NH₃, H-NH₃, H-OH), 3.76 (s, 2H, H-3, H-7), 3.59 (s, 2H, H-12, H-25), 3.36 (s, H-H₂O), 3.22–3.13 (m, 3H, H-26a, H-26b, H-29a), 3.12–3.04 (m, 1H, H-29b), 2.49 (s, H-DMSO), 2.35 (t, *J* = 10.3 Hz, 2H, H-23), 2.29–2.08 (m, 2H, H-15a, H-16a), 1.95 (tdt, *J* = 33.5, 14.0, 6.1 Hz, 2H, H-22), 1.74 (q, *J* = 12.6, 11.2 Hz, 4H, H-2a, H-4a, H-6a, H-11a), 1.62 (d, *J* = 15.1 Hz, 2H, H-15b, H-16b), 1.42 (t, *J* = 12.1 Hz, 3H, H-2b, H-11b, H-1a), 1.34 (t, *J* = 12.6 Hz, 2H, H-4b, H-6b), 1.23 (q, *J* = 9.4, 5.9 Hz, 2H, H-1b, H-20), 1.12 (q, *J* = 9.9 Hz, 2H, H-5, H-8), 0.90 (d, *J* = 6.9 Hz, 3H, H-9, H-14, H-17), 0.79 (s, 5H, H-19, H-21), 0.56 (d, *J* = 7.9 Hz, 4H, H-18, H-19). ¹³C NMR (126 MHz, DMSO-*d*₆) δ 177.42 (C, C-30), 176.89 (C, C-28), 172.02 (C, C-24), 71.05 (CH, C-12), 70.48 (CH, C-3), 66.29 (CH, C-7), 50.16 (C, C-27), 46.15 (C, C-13), 45.77 (CH, C-17), 41.55 (CH, C-14), 41.40 (CH, C-25), 39.52 (dp, *J* = 42.2, 21.0 Hz, C-DMSO), 38.87 (CH, C-5), 38.29 (CH, C-8), 35.34 (CH₂, C-4), 35.28 (CH₂, C-6), 34.93 (C, C-10), 34.43 (CH₂, C-1), 33.39 (CH, C-20), 32.49 (CH₂, C-23), 31.77 (CH₂, C-26), 30.43 (CH₂, C-29), 28.60 (CH₂, C-22), 27.34 (CH₂, C-2), 26.25 (CH₂, C-11), 25.36 (CH, C-9), 24.51 (CH₂, C-16), 22.86 (CH₂, C-15), 22.67 (CH₃, C-21), 17.18 (CH₃, C-19), 12.40 (CH₃, C-18). All the data above were in good agreement with the structure of CP-CA. The synthesis strategy was highly innovative. Instead of using CP as a raw material, CP-CA was synthesized simultaneously, meaning that the synthesis of CP and the CA modification occurred concurrently. In addition, CP is more expensive than cis-Pt(NH₃)₂I₂; therefore, using cis-Pt(NH₃)₂I₂ can significantly save the synthesis cost, which is important for future further development in future.

2.2. Cell Toxicity

The cell viabilities (%) of normal human liver cell HL7702 and human liver cancer cell Huh7 are shown in Figure 2 after treatment with different concentrations of CP-CA and CP, respectively, for 72 h. It could be seen that the survival of cells decreased with the increase in the concentrations of CP-CA and CP. The half-maximal inhibitory concentration (IC₅₀) data are shown in Table 1. For HL7702 and Huh7, there was no significant difference between CP-CA and CP (*p* > 0.05), showing the similar cell toxicities of the two compounds. It was interesting that for CP, there was significant difference between HL7702 and Huh7 (*p* < 0.01), showing higher toxicity on normal human liver cells compared to on liver cancer cells; however, for CP-CA, there was no significant difference between HL7702 and Huh7 (*p* > 0.05). Further investigation on the mechanism should be conducted in future study.

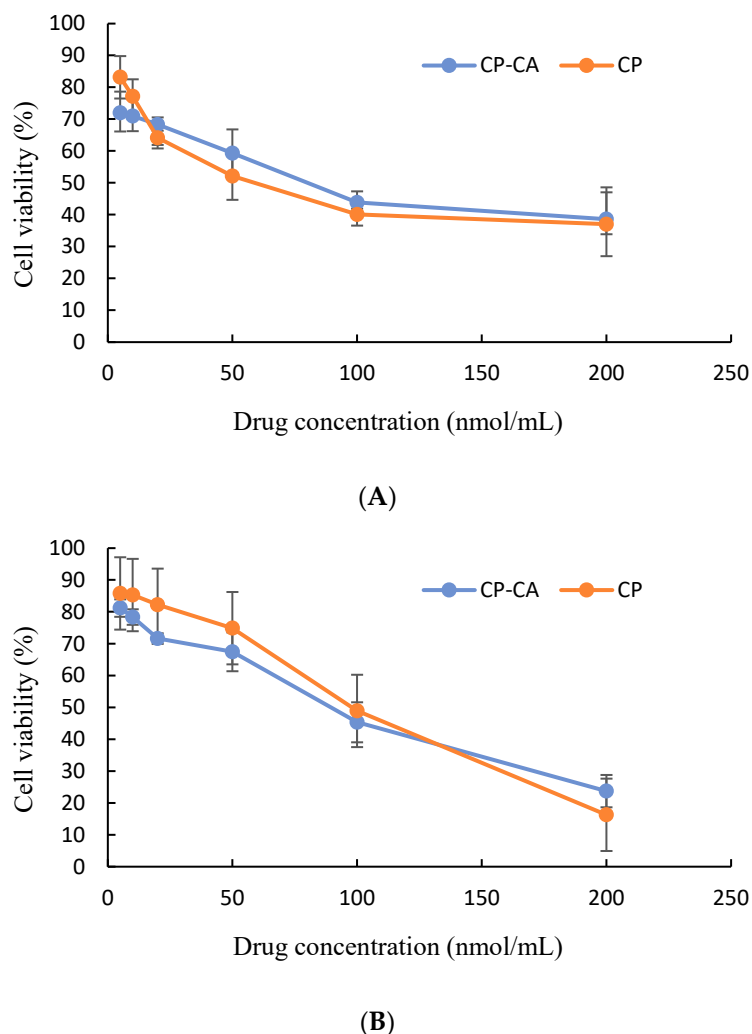


Figure 2. Cell toxicity of CP-CA and CP on normal human liver cell HL7702 (A) and human liver cancer cell Huh7 (B).

Table 1. IC 50 of CP-CA and CP against cell lines HL7702 and Huh7 (nmol/mL, $n = 3$).

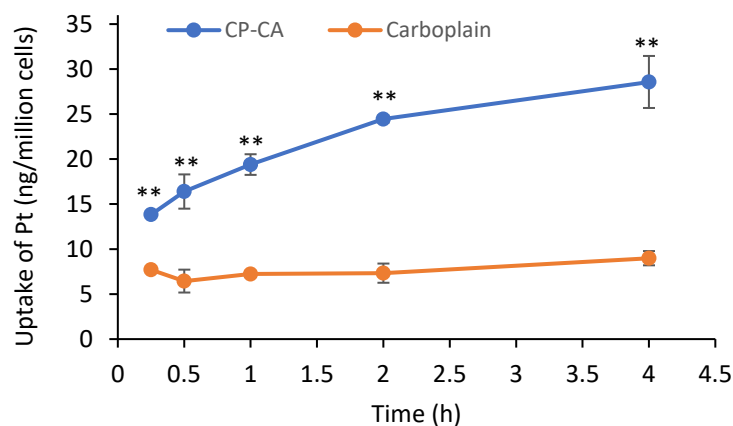
Cell Line	CP-CA	CP
HL7702	81.91 ± 7.45	72.32 ± 8.07
Huh7	89.78 ± 9.62	98.87 ± 10.24 **

t-test, compared with HL7792, ** $p < 0.01$.

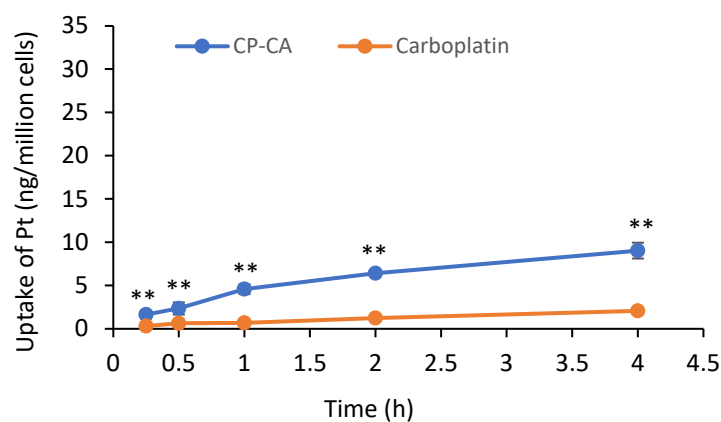
2.3. In Vitro Cell Uptake

After culturing with CP-CA and CP at a final concentration of 10 nmol/mL for 15 min, 30 min, 1 h, 2 h, and 4 h, Huh7 and HL7702 cells were washed twice with PBS and collected. The content of Pt in each sample was quantitatively assessed using ICP-MS. The results of Pt uptake of CP-CA and CP by the cells are shown in Figure 3. For both Huh7 and HL7702 cells, CP-CA had a significantly higher uptake of Pt compared with that of CP at each time point ($p < 0.01$), indicating that the modification with cholic acid had significant contribution to the improvement of Pt uptake, which strongly confirmed our assumption and design. It was also interesting that the Huh7 cell line exhibited a higher uptake of Pt compared with that of the HL7702 cell line ($p < 0.01$), regardless of whether the Pt-based drug was CP or CP-CA. This differential uptake could suggest a selective or targeted interaction of CP-CA and CP with liver cancer cells over normal liver cells, which could have significant implications for the clinical application and safety profile of these treatments. There has been no report on the expression difference of bile acid receptors between the Huh7 and

HL7702 cell lines. From a chemical point of view, the molecule of CA has two different groups: hydrophilic (α -OH and α -COOH) and hydrophobic (β -CH₃ and hydrocarbon nucleus) ones. The groups of -OH, -COOH, and -CH₃ are located on the two opposite sides of the molecule. Therefore, CA can work as a surfactant to increase the binding ability of CP-CA to the cell membrane and improve the passive diffusion of CP-CA into the cells. Another more important reason, from a molecular biological point of view, is possibly related to the function of the bile acid receptors in the cell membrane mentioned above, which can actively transport CP-CA into the cells. Further investigation will be warranted in future research to reveal the mechanisms of Pt-based anticancer drugs and the transport of bile acids.



(A)



(B)

Figure 3. Uptake of Pt in CP-CA and CP by human liver cancer cell Huh7 (A) and normal human liver cell HL7702 (B) ($n = 3$) indicates that CP-CA can be more easily transferred into HL7702 and Huh7 cells compared with CP (** t -test, $p < 0.01$).

2.4. PK Study

2.4.1. Plasma Protein Binding Rate (PPBR)

The PPBRs of CP-CA and CP were $(81.0 \pm 4.5) \%$ and $(18.9 \pm 3.9) \%$, respectively, showing that CP-CA had a higher binding ability with plasma protein compared with CP. It has been known that the protein-binding behavior of a drug in blood is important because it influences the transport, distribution, and toxicity of the drug. It was reported that different Pt-based drugs had different PPBRs. For example, for cisplatin, CP, and oxaliplatin, the PPBR values to rat plasma protein were 96%, 15%, and 80%, correspondingly, leading to the difficulties involved with predicting the tissue concentrations of cisplatin and oxaliplatin

from their plasma concentrations. On the contrary, it is possible to conduct therapeutic drug monitoring for CP [32]. Therefore, further research should be carried out to investigate the reversibility or irreversibility of CP-CA to plasma protein and whether the binding of CP-CA to protein affects the protein binding site of other drugs.

2.4.2. PK Study

The rats were intravenously injected CP-CA and CP via the tail vein, respectively, at the same dose of 2.28 mg/kg body weight calculated by Pt. based on the Pt quantification of the plasma samples; the PK concentration–time profiles of Pt for CP-CA and CP are shown in Figure 4. It showed that the concentrations of Pt for CP-CA at all time points, even at the first time point (0.033 h), were much higher than those of Pt for CP, indicating the significantly different distribution of CP-CA and CP after intravenous administration. The PK parameters were obtained using PK software DAS 2.0. The metabolic process of Pt conformed with a two-compartment model, meaning that drugs entered the central compartment initially and were instantaneously and evenly distributed. Subsequently, they gradually dispersed into the peripheral compartment. The major PK parameters of Pt for CP-CA and CP such as elimination half-life ($t_{1/2}$), area under the curve (AUC), clearance (CL), apparent volume of distribution (Vd), and mean retention time (MRT) are shown in Table 2. The AUC means the degree of drug exposure and accumulation which is closely related to bioavailability. For CP-CA, both AUC_{0-t} (47.00 ± 8.20 mg/L·h) and $AUC_{0-\infty}$ (54.46 ± 9.40 mg/L·h) data on Pt were significantly higher than those on CP (9.31 ± 1.86 mg/L·h and 11.15 ± 2.90 mg/L·h, respectively) ($p < 0.01$), indicating that the plasma exposure of CP-CA was significantly higher than that of CP. The CL_1 , Vd_1 , and Vd_2 data on Pt for CP-CA were significantly lower than those on CP ($p < 0.01$), and the MRT_{0-t} of Pt for CP-CA (3.38 ± 0.37 h) was significantly higher than that for CA (1.92 ± 0.68 h) ($p < 0.01$), indicating that CP-CA was eliminated more slowly after administration. It was possibly related to a higher PPBR and could strongly support the higher AUC of Pt for CP-CA compared to that for CP.

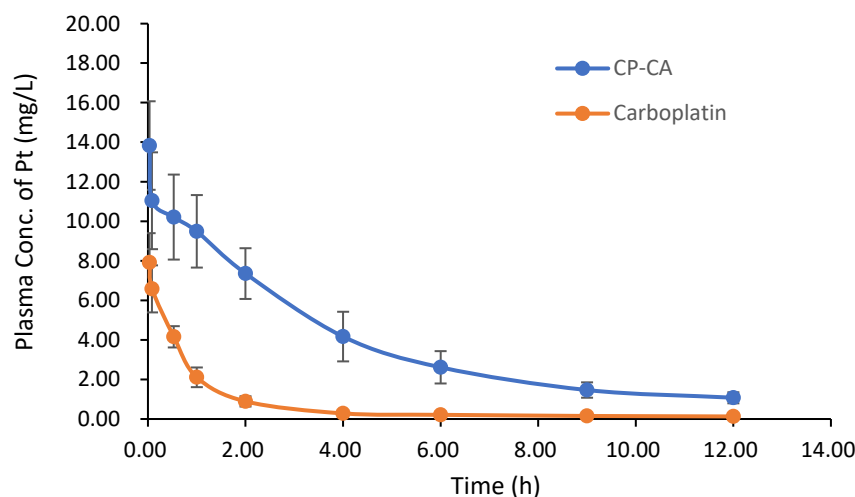


Figure 4. Plasma concentration–time profiles of Pt of CP-CA and CP after i.v. administration to rats with a single dose of 2.28 mg/kg calculated by Pt (equal to 11.7 mmol/kg of CP-CA and CP) ($n = 6$).

Table 2. PK parameters of Pt of CP-CA and CP in plasma after i.v. administration to rats with a single dose of 2.28 mg/kg calculated by Pt (equal to 11.7 mmol/kg of CP-CA and CP) (mean \pm SD, $n = 6$).

Parameters	CP	CP-CA
$t_{1/2\alpha}$ (h)	0.44 ± 0.09	0.73 ± 0.58
$t_{1/2\beta}$ (h)	5.51 ± 2.40	4.80 ± 1.97
Vd_1 (L/kg)	0.27 ± 0.05	$0.16 \pm 0.05^{**}$

Table 2. Cont.

Parameters	CP	CP-CA
V _{d2} (L/kg)	0.64 ± 0.28	0.10 ± 0.05 **
CL ₁ (L/h/kg)	0.25 ± 0.07	0.04 ± 0.01 **
CL ₂ (L/h/kg)	0.16 ± 0.06	0.33 ± 0.62
AUC _{0-t} (mg/L·h)	9.31 ± 1.86	47.00 ± 8.20 **
AUC _{0-∞} (mg/L·h)	11.15 ± 2.90	54.46 ± 9.40 **
K ₁₀ (1/h)	0.94 ± 0.35	0.32 ± 0.17 **
K ₁₂ (1/h)	0.58 ± 0.18	4.04 ± 8.82
K ₂₁ (1/h)	0.27 ± 0.12	3.19 ± 5.31
MRT _{0-t} (h)	1.92 ± 0.68	3.38 ± 0.37 **
MRT _{0-∞} (h)	4.92 ± 2.51	5.56 ± 0.68

t-test, ** *p* < 0.01 compared to the data of CP.

2.5. Tissue Distribution

The tissue distribution of Pt in the heart, liver, spleen, lung, kidney, and ovary for CP-CA and CP at four different time points (0.083 h, 2 h, 4 h, and 8 h) is shown in Figure 5. In the heart, Pt concentration for CP-CA was significantly higher than that for CP at each time point (*p* < 0.01), although the overall levels were not so high like in other tissues. In the liver, Pt concentration for CP-CA was significantly higher than that for CP at each time point (*p* < 0.01). The concentrations were 5.89, 6.88, 7.59, and 10.31 times higher at 0.083 h, 2 h, 4 h, and 8 h, respectively, indicating that the modification with cholic acid could significantly enhance the liver distribution of Pt. In the spleen, Pt concentration for CP-CA was also significantly higher than for CP at any time point (*p* < 0.01) and consistently high throughout the 8 h period. In the lung, Pt concentration for CP-CA was significantly higher at 0.083 h, 2 h, and 8 h (*p* < 0.01) compared with that for CP. For both CP-AC and CP, Pt concentration was highest at 0.083 h and then rapidly decreased. In the kidney, Pt concentration for CP was the highest compared with that in any other tissues, showing it could be gathered in the kidney very fast after administration and excreted mainly through the kidney. Pt concentration for CP-CA was about only 27.2% of that for CP, but significantly higher at 2 h, 4 h, and 8 h (*p* < 0.05, *p* < 0.01). In the ovary, Pt concentration for CP-CA had no significant difference at 0.083 h compared with that for CP (*p* > 0.05), but higher at 2 h, 4 h, and 8 h (*p* < 0.05), although the total levels for either CP-CA or CP were not so high.

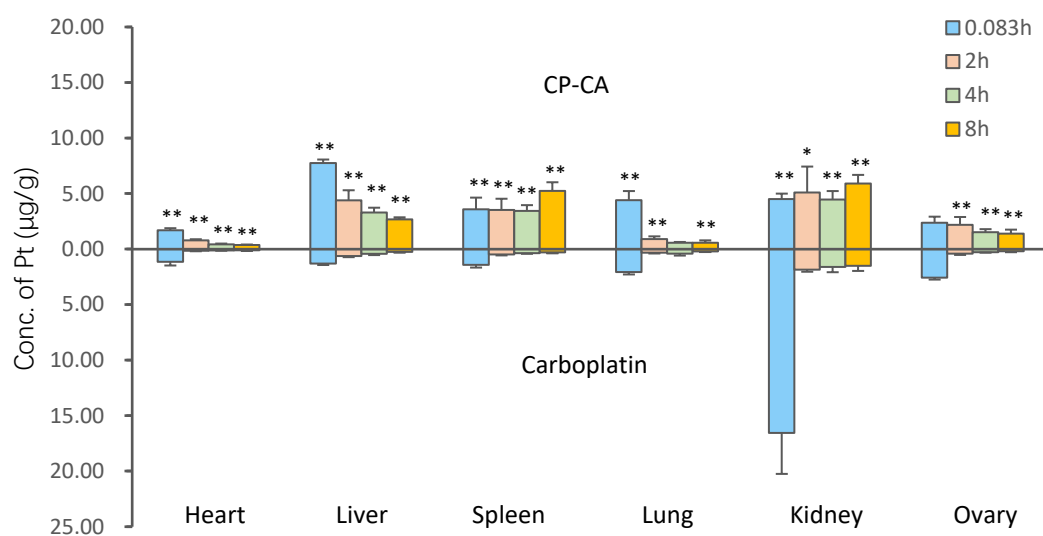


Figure 5. Tissue distribution of Pt for CP-CA and CP after i.v. administration to rats at a single dose of 2.28 mg/kg calculated by Pt (equal to 11.7 mmol/kg of CP-CA and CP) (*n* = 6) (*t*-test, * *p* < 0.05, ** *p* < 0.01, compared with CP).

In order to compare the drug exposure in different tissues between CP-CA and CP, the AUC_{0-t} data on Pt were calculated and the results are shown in Figure 6. In all tissues, CP-CA had a significantly higher AUC_{0-t} of Pt than CP ($p < 0.05$, $p < 0.01$). For CP, the AUC_{0-t} of Pt in the kidney was the largest compared with that of the other tissues, while for CP-CA, the AUC_{0-t} of Pt in the liver was the largest but it was also very high in the spleen. The results that CP-CA had a higher AUC_{0-t} of Pt than CP could be caused by its higher PPBR or other complicated factors, and further molecular mechanisms should be performed in future.

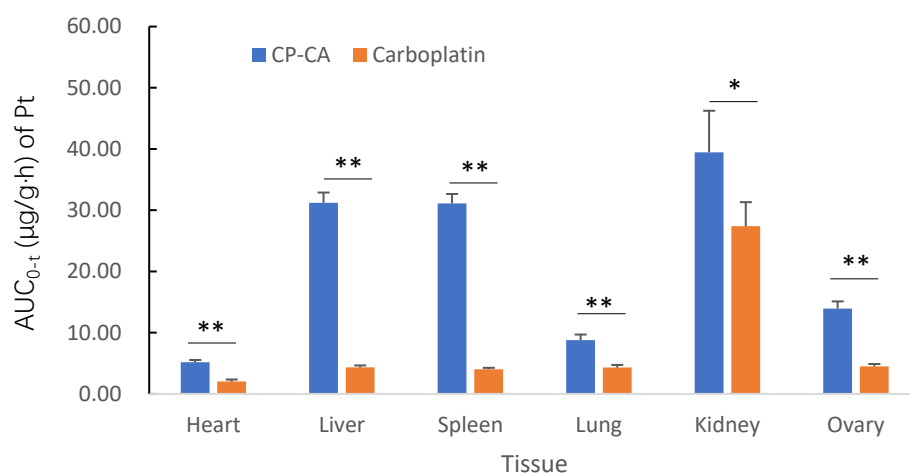


Figure 6. AUC_{0-t} ($\mu\text{g/g}\cdot\text{h}$) of Pt of CP-CA and CP in tissues after i.v. administration to rats with a single dose of 2.28 mg/kg calculated by Pt (equal to 11.7 mmol/kg of CP-CA and CP) ($n = 6$) (t -test, * $p < 0.05$, ** $p < 0.01$, compared to the data of CP).

According to the plasma PK study and tissue distribution, it could be concluded that the distribution of Pt in the liver could be significantly improved after intravenous administration of CP-CA compared with CP for which Pt was mainly distributed in the kidney. The distribution of Pt for CP-CA in the spleen was also high, which was possibly caused by rich blood flow and macrophages and related to its high plasma concentration. Furthermore, it was evident that CP-CA had greater drug exposure than CP, as indicated by the higher C_{0-t} values observed in both plasma and tissues. It has been widely known that the clinical efficacy is mainly decided by the concentration of Pt; therefore, in the clinical application of CP-CA, the dose can be reduced to maintain a therapeutic effect and minimize toxicity and side effects.

The PK and tissue distribution profiles of Pt for CP-CA were similar to those of LLC-202, a cholic acid-conjugated oxaliplatin we have developed and reported (Figure 7A), which also uses 3- NH_2 -cyclobutane-1,1-dicarboxylate as a linker between the oxaliplatin analog and CA moiety, and CA is strongly bonded to the linker via an amide bond. The PK results showed that the AUC_{0-t} could be improved about five times for both CP-CA compared with CP and LLC-202 compared with oxaliplatin. The tissue distribution experiment showed that both CP-CA and LLC-202 were mainly distributed and accumulated in the liver after intravenous administration to rats, revealing the liver-targeting profile. Therefore, the results of both CP-CA and LLC-202 could strongly support the modification strategy of Pt-based antitumor drugs by CA conjugation using 3- NH_2 -cyclobutane-1,1-dicarboxylate as a linker. The structure of CP-CA is different from the reported cholic acid-carboplatin compound (CarboChAPt), with which CA is linked via an alkyl spacer to a carboplatin analog [33] (Figure 7B). In general, the cytostatic activity of CarboChAPt is similar to that of the parent compound and strongly influenced by the length of the alkyl chain spacer separating the drug and transport fragments, with the ones with long-chain spacers being more toxic than the parent complexes. It can be explained that a large group linked via an alkyl spacer will increase the steric hindrance to the coordination of Pt with N7 on DNA

purines, thereby affecting the anticancer activity. It is a pity that there has been no further report on its in vivo activity or PK and tissue distribution profiles.

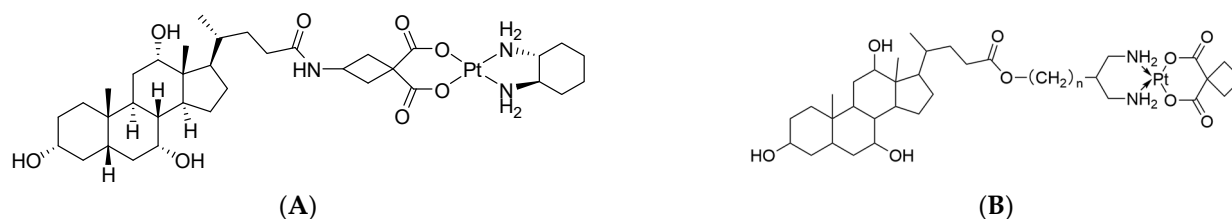


Figure 7. Chemical structures of LLC-202 (A) and CarboChAPt (B).

This present paper mainly focuses on the comparison of PK profiles, tissue distribution, and cell uptake of Pt for CP-CA and the parent drug CP. To further support the proposed hypotheses, more and deeper explorations into the molecular mechanism of CP-CA transport across various cell types, drug resistance, in vitro activities against cancer cells, and in vivo anticancer activities in animal models should be performed, which have been partially completed, and more comprehensive research will be reported later.

3. Materials and Methods

3.1. Materials and Reagents

CP was provided by the Kunming Guiyan Pharmaceutical Co (Kunming, China). Distilled and deionized water was prepared with a Milli-Q Academic System (Molsheim, France). Pt standard solution (GSB04-1744-2004, National Center of Standard Metals, Ministry of Metallurgy, Beijing, China) was provided by the Analysis Center, Tsinghua University. The solution was freshly diluted with a 2% HNO₃ solution before detection. Solutions of 68% (*w/w*) HNO₃ (ultra-pure grade) and 30% (*w/w*) H₂O₂, NaHCO₃, and AgNO₃ were purchased from Beijing Chemical Factory (Beijing, China). Dialysis tube (3500 D) was purchased from Beijing Solarbio Science & Technology Co., Ltd. (Beijing, China). 3-cholylamide-1,1-cyclobutanedicarboxylic acid, and diiododiammine platinum (NH₃PtI₂) were purchased from Alfa Aesar (Shanghai, China).

Sixty female Sprague Dawley (SD) rats (200 ± 20 g) were purchased from Beijing Weitong Lihua Experimental Animal Co., Ltd. (Beijing, China). All the animals were kept in the Centre of Experimental Animals of Tsinghua University (Beijing, China), in a normally controlled breeding room (temperature: 20 ± 2 °C, humidity: 60 ± 5%, 12 h dark/light cycle) with standard laboratory food and water prior to the experiments. The rats were fasted 24 h before the administration of the tested drugs but had free access to water. The experimental procedures were performed according to the Guide for the Care and Use of Laboratory Animals, Tsinghua University.

3.2. Chemical Synthesis of CP-CA

The synthesis of CP-CA is illustrated in Figure 8. Disodium 3-cholylamide-1,1-cyclobutanedicarboxylate was prepared via the acid–base neutralization reaction at room temperature between 3-cholylamide-1,1-cyclobutanedicarboxylic acid, and NaHCO₃. The quantitative reaction of AgNO₃ at 40–45 °C with a commercially available platinum compound, *cis*-Pt(NH₃)₂I₂, gave rise to an intermediate which was converted to the desired product CP-CA by mixing with 3-cholylamide-1,1-cyclobutanedicarboxylate. The elemental composition, molecular weight, and structure of CP-CA were confirmed by the elemental composition analysis, through HRESI⁺-MS, IR, ¹HNMR, ¹³CNMR, and 2D NMR spectra including heteronuclear single-quantum coherence (HSQC) and heteronuclear multiple-bond correlation (HMBC).

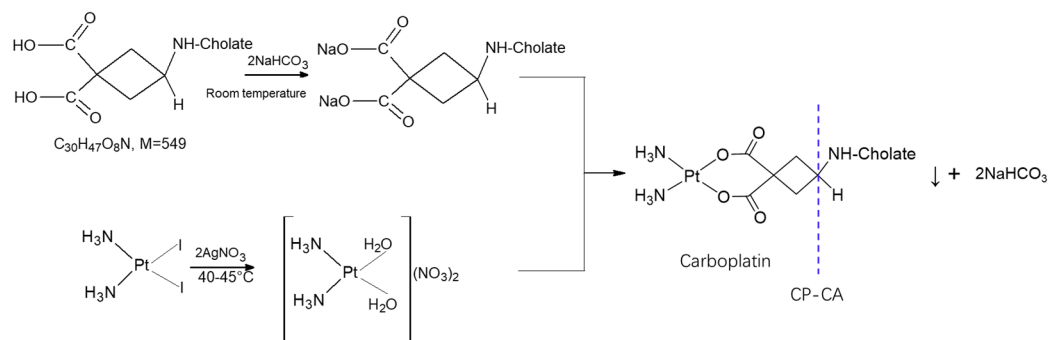


Figure 8. Synthesis routes and conditions of CP-CA.

3.3. Cell Toxicity

Normal human liver cell line HL7702 and human liver cancer cell line Huh7 were provided by Prof. Ligong Chen (School of Pharmaceutical Sciences, Tsinghua University, China). The cells in a logarithmic growth stage were seeded into 96-well plates with 4000 cells per well. After incubation at 37 °C in a 5% CO₂ environment for 24 h, the cells were exposed to CP-CA or CP at concentrations of 5, 10, 20, 50, 100, and 200 nmol/mL. A control group, treated with the vehicle alone, was incorporated to serve as a baseline for comparison. The experiment was conducted in triplicate. After drug exposure for 72 h, the cell viability was detected by a methyl thiazolyl tetrazolium (MTT) assay, and the IC₅₀ values of the compounds were calculated according to the dose–response curves using SPSS 24 software.

3.4. Instrument Conditions for Bio-Samples

The bio-samples for cell uptake, plasma pharmacokinetics (PKs), and tissue distribution were analyzed using DRC-e ICP-MS (Waltham, MA, USA) based on the methods developed and optimized before [31]. The analytes were automatically introduced into the ionization source of the mass spectrometer by the autosampler, ensuring precise and reproducible sample injection. The radiofrequency power of the instrument was 1.2 kW. The flow rates were set as follows: 15 L/min for the cooling gas, 0.7 L/min for the atomizer gas, and 1.0 L/min for the auxiliary gas.

3.5. In Vitro Cell Uptake Kinetics

CP-CA and CP were dissolved in DMSO at a concentration of 2 µmol/mL as the initial solution. The Huh7 and HL7702 cells were cultivated at 37 °C in a 5% CO₂ environment, using Dulbecco's modified eagle medium (DMEM) supplemented with 10% fetal bovine serum (FBS). The cells were seeded into 6-well plates, at a density of 2 million cells per well and incubated. After 24 h, the cells were exposed to the culture medium diluted compound at a final concentration of 10 nmol/mL (DMSO concentration of 0.5%). After incubation with the compound for 15 min, 30 min, 1 h, 2 h, and 4 h, the cells were gently washed twice with PBS to remove any residual compound and subsequently collected at each time frame for further analysis. The experiment was performed in triplicate. The viability of cells was assessed using the MTT method concurrently with the experiment, and the resulting viability data were used to normalize the uptake data on Pt by the cells.

The treatment protocol for the cell samples was as follows: the cells collected at each time point were transferred into a beaker, followed by the addition of 3 mL of concentrated HNO₃ to facilitate sample digestion. The beaker was placed on a hot plate and heated with reflux at 180 °C for 1 h until complete dissolution was achieved. Once the solution had cooled to room temperature, 0.6 mL of H₂O₂ was added, followed by heating the beaker to induce complete precipitation of the sample. The liquid was carefully evaporated to a final volume of 0.5 mL, after which the residue was diluted with a 2% HNO₃ solution to a final volume of 10 mL for Pt determination. The concentration of Pt in each sample was measured by ICP-MS.

3.6. PK Study

3.6.1. Plasma Protein Binding Rate (PPBR)

Twenty-five mg of CP-CA was accurately weighed and diluted with PBS (pH 7.4) to a final volume of 500 mL, from which 150 mL was taken as the dialysis external solution. In total, 1 mL of blank plasma was transferred into a dialysis bag and suspended in a beaker containing 150 mL of the dialysis external solution and then equilibrated at 4 °C for 48 h. The Pt concentrations of Pt in the dialysis external and internal solutions (C_{out} , C_{in}) were measured using ICP-MS, respectively, and the PPBR was calculated by $(C_{in} - C_{out})/C_{in} \times 100\%$. The PPBR of CP was also determined following the same procedure. For each sample, triplicate measurements were performed.

3.6.2. PK Study

CP-CA was dissolved in a mixed solution comprising 5% glucose and 20% polyethylene glycol 400 (PEG-400) to obtain a final concentration of 0.908 mg/mL (1.17 $\mu\text{mol/mL}$), and CP was dissolved in 0.5% glucose to a final concentration of 0.434 mg/mL (1.17 $\mu\text{mol/mL}$).

Twelve rats were divided into two groups of six rats each: one for PK study of CP-C and the other one for CP. The rats were intravenously administered by tail vein with the drug solutions. For CP and CP-CA, the key active element is Pt. For the comparison of the activities, the same amount of Pt for CP and CP-CA should be used. The injection doses of CP-CA and CP were 9.08 mg/kg and 4.34 mg/kg body weight, respectively, both equal to 11.7 mmol/kg (2.28 mg/kg for Pt). Blood samples (0.3 mL) were collected from the ophthalmic venous plexus of each rat into heparinized tubes at 0.033, 0.16, 0.5, 1, 2, 4, 6, 9, and 12 h after administration. The blood sample was centrifuged at 4 °C and $11,000 \times g$ for 10 min to separate the plasma. The resulting plasma was then transferred into a clean tube and stored at 4 °C for subsequent analysis.

The treatment protocols for the plasma samples were as follows: an aliquot of 0.1 mL plasma was transferred into a beaker, followed by the addition of 3 mL of concentrated HNO_3 to facilitate sample digestion. The beaker was placed on a hot plate and heated with reflux at 180 °C for 1 h until complete dissolution was achieved. Once the solution had cooled to room temperature, 0.6 mL of H_2O_2 was added, followed by heating the beaker to induce complete precipitation of the sample. The liquid was carefully evaporated to a final volume of 0.5 mL, after which the residue was diluted with a 2% HNO_3 solution to a final volume of 10 mL for Pt determination. The concentration of Pt in each sample was measured by ICP-MS.

A series of standard Pt solutions were prepared and determined, with concentrations ranging from 0 to 400 ng/mL, for calibration and quantification purposes. Based on the calibration curve obtained, the Pt concentration of each sample was calculated according to the linear regression equation. For each sample, duplicate measurements were performed.

All data were presented as the mean \pm standard deviation (SD). PK parameters such as elimination half-life ($t_{1/2}$), distribution volume (V), clearance (CL), mean retention time (MRT), and area under concentration–time curve (AUC) were calculated with DAS 2.0 software (Mathematical Pharmacology Professional Committee of China, Shanghai, China). Statistical analysis was conducted using Microsoft Excel 2016. The differences in indices above between CP-CA and CP groups were analyzed by student's *t*-test. A two-tailed *p* value of less than 0.05 was considered to indicate statistical significance.

3.7. Tissue Distribution

Twenty-four rats were evenly divided into 4 groups with six rats per group. CP-CA was administered intravenously via the tail vein at a dosage equivalent to that used in the PK study. At 0.083, 2, 4, and 8 h after administration, one group of animals was mildly sedated using diethyl ether and humanely euthanized by cervical dislocation. Tissue samples, comprising the heart, liver, spleen, lung, kidney, and ovary, were immediately excised and rinsed with a 0.9% saline solution. After blotting with filter paper, they were weighed, finely chopped with a sterile blade, and stored at -80 °C till treatment for ICP-MS

analysis. The tissue distribution study of CP was conducted using an additional 24 rats, administered at the same dosage as employed in the PK study.

The tissue samples were processed using a method analogous to that for plasma samples, with the exception that 2 mL of concentrated HNO₃ was applied per 0.1 g of tissue samples during the digestion phase. According to the calibration curve obtained, the Pt concentration of each sample was calculated according to the linear regression equation. For each sample, duplicate measurements were performed.

All data were presented as mean \pm standard deviation (SD). The mean values were compared with a *t*-test between CP-CA and CP groups by Microsoft Excel 2016, and a value of *p* < 0.05 was considered statistically significant.

4. Conclusions

In this paper, a novel cholic acid-conjugated carboplatin (CP-CA) was synthesized as a prodrug of carboplatin (CP) for liver cancer. Based on cell toxicity and cell uptake investigation, PK and tissue distribution profiles of Pt for CP-CA were determined and compared with those for CP by measuring Pt in rats after i.v. administration of a single dose. The results indicated that following i.v. administration, CP-CA was mainly distributed in the liver, which was significantly different from the renal-centric distribution for CP. Furthermore, the higher systemic and tissue exposure to CP-CA implied that a reduced dosage regimen could be viable for future clinical applications, potentially minimizing the risk of toxicity and adverse side effects.

Supplementary Materials: The following supporting information can be downloaded at <https://www.mdpi.com/article/10.3390/inorganics12070184/s1>, (1) element composition analysis, (2) ESI MS, (3) HRESI MS, (4) IR, (5) ¹HNMR, (6) ¹³CNMR, (7) HSQC, (8) HMBC.

Author Contributions: Chemical synthesis, A.G. and J.J.; animal and cell experiment and sample determination, Y.L. and F.H.; data analysis, X.F. and Y.H.; design, supervision, and review, Z.W., W.L. and Q.L. All authors have read and agreed to the published version of the manuscript.

Funding: This work was supported by the National Natural Science Foundation of China (21661018), Yunnan Provincial Science and Technology Department of China (202001AT070090, 202102AA310026), and State Key Laboratory of Advanced Technologies for Comprehensive Utilization of Platinum Metals (SKL-SPM-201802).

Institutional Review Board Statement: The animal study protocol was approved by the Ethics Committee of Tsinghua University (protocol code 14-LQF2.G22-1, 25 November 2022).

Informed Consent Statement: Not applicable.

Data Availability Statement: The original contributions presented in this study are included in the article and further inquiries can be directed to the corresponding authors.

Acknowledgments: The authors would like to thank Experimental Animal Center, Tsinghua University, for supporting and providing facilities to conduct the animal work.

Conflicts of Interest: The authors declare no conflicts of interest.

References

1. Siegel, R.L.; Miller, K.D.; Jemal, A. Cancer statistics. *CA Cancer J. Clin.* **2020**, *70*, 7–30. [[CrossRef](#)] [[PubMed](#)]
2. Rungay, H.; Arnold, M.; Ferlay, J.; Lesi, O.; Cabasag, C.J.; Vignat, J.; Laversanne, M.; McGlynn, K.A.; Soerjomataram, I. Global burden of primary liver cancer in 2020 and predictions to 2040. *J. Hepatol.* **2022**, *77*, 1598–1606. [[CrossRef](#)] [[PubMed](#)]
3. Bedard, P.L.; Hyman, D.M.; Davids, M.S.; Siu, L.L. Small molecules, big impact: 20 years of targeted therapy in oncology. *Lancet* **2020**, *395*, 1078–1088. [[CrossRef](#)] [[PubMed](#)]
4. Kelland, L. The resurgence of platinum-based cancer chemotherapy. *Nat. Rev. Cancer* **2007**, *7*, 573–584. [[CrossRef](#)] [[PubMed](#)]
5. Navo, M.; Kunthur, A.; Badell, M.L.; Coffey, L.W.; Markman, M.; Brown, J.; Smith, J.A. Evaluation of the incidence of carboplatin hypersensitivity reactions in cancer patients. *Gynecol. Oncol.* **2006**, *103*, 608–613. [[CrossRef](#)] [[PubMed](#)]
6. Markman, M.; Kennedy, A.; Webster, K.; Elson, P.; Peterson, G. Clinical features of hypersensitivity reactions to carboplatin. *J. Clin. Oncol.* **1999**, *17*, 1141–1145. [[CrossRef](#)] [[PubMed](#)]

7. Paksoy, N.; Khanmammadov, N.; Doğan, İ.; Ferhatoğlu, F.; Yildiz, A.; Ak, N.; Aydiner, A. Toxicity management and efficacy of carboplatin desensitization therapy for recurrent epithelial ovarian carcinoma: A real-world study. *Medicine* **2022**, *101*, e31726. [[CrossRef](#)]
8. Schmitt, A.; Gladieff, L.; Laffont, C.M.; Evrard, A.; Boyer, J.C.; Lansiaux, A.; Bobin-Dubigeon, C.; Etienne-Grimaldi, M.-C.; Boisdron-Celle, M.; Mousseau, M.; et al. Factors for hematopoietic toxicity of carboplatin: Refining the targeting of carboplatin systemic exposure. *J. Clin. Oncol.* **2010**, *28*, 4568–4574. [[CrossRef](#)] [[PubMed](#)]
9. Johnstone, T.C.; Suntharalingam, K.; Lippard, S.J. The next generation of Platinum drugs: Targeted Pt (II) agents, nanoparticle delivery, and Pt (IV) prodrugs. *Chem. Rev.* **2016**, *116*, 3436–3486. [[CrossRef](#)]
10. Sievanen, E. Exploitation of bile acid transport systems in prodrug design. *Molecules* **2007**, *12*, 1859–1889. [[CrossRef](#)]
11. Patra, M.; Johnstone, T.C.; Suntharalingam, K.; Lippard, S.J. A potent glucose-platinum conjugate exploits glucose transporters and preferentially accumulates in cancer cells. *Angew. Chem. Int. Ed. Engl.* **2016**, *55*, 2550–2554. [[CrossRef](#)] [[PubMed](#)]
12. Weitman, S.D.; Lark, R.H.; Coney, L.R.; Fort, D.W.; Frasca, V.; Zurawski, V.R., Jr.; Kamen, B.A. Distribution of the folate receptor GP38 in normal and malignant cell lines and tissues. *Cancer Res.* **1992**, *52*, 3396–3401. [[PubMed](#)]
13. Trauner, M.; Boyer, J.L. Bile salt transporters: Molecular characterization, function, and regulation. *Physiol. Rev.* **2003**, *83*, 633–671. [[CrossRef](#)]
14. Kramer, W.; Wess, G. Bile acid transport systems as pharmaceutical targets. *Eur. J. Clin. Investig.* **1996**, *26*, 715–732. [[CrossRef](#)]
15. Kramer, W.; Wess, G.; Schubert, G.; Bickel, M.; Girbig, F.; Gutjahr, U.; Kowalewski, S.; Baringhaus, K.H.; Enhsen, A.; Glombik, H.; et al. Liver-specific drug targeting by coupling to bile acids. *J. Biol. Chem.* **1992**, *267*, 18598–18604. [[CrossRef](#)]
16. Meijer, D.K. Drug targeting to the liver with bile acids: The “Trojan horse” resurrected? *Hepatology* **1993**, *17*, 945–948. [[CrossRef](#)] [[PubMed](#)]
17. Monte, M.J.; Dominguez, S.; Palomero, M.F.; Macias, R.I.; Marin, J.J. Further evidence of the usefulness of bile acids as molecules for shuttling cytostatic drugs toward liver tumors. *J. Hepatol.* **1999**, *31*, 521–528. [[CrossRef](#)]
18. Qian, S.; Wu, J.B.; Wu, X.C.; Li, J.; Wu, Y. Synthesis and characterization of new liver targeting 5-fluorouracil-cholic acid conjugates. *Arch. Pharm.* **2009**, *342*, 513–520. [[CrossRef](#)]
19. Chen, D.Q.; Wang, X.; Chen, L.; He, J.X.; Miao, Z.H.; Shen, J.K. Novel liver-specific cholic acid-cytarabine conjugates with potent antitumor activities: Synthesis and biological characterization. *Acta Pharmacol. Sin.* **2011**, *32*, 664–672. [[CrossRef](#)]
20. Dominguez, M.F.; Macias, R.I.; Izco-Basurko, I.; de La Fuente, A.; Pascual, M.J.; Criado, J.M.; Monte, M.J.; Yajeya, J.; Marin, J.J. Low in vivo toxicity of a novel cisplatin-ursodeoxycholic derivative (Bamet-UD2) with enhanced cytostatic activity versus liver tumors. *J. Pharmacol. Exp. Ther.* **2001**, *297*, 1106–1112.
21. Zimmer, A.; Gespach, C. Bile acids and derivatives, their nuclear receptors FXR, PXR and ligands: Role in health and disease and their therapeutic potential. *Anticancer Agents Med. Chem.* **2008**, *8*, 540–563. [[CrossRef](#)] [[PubMed](#)]
22. Schaap, F.G.; Trauner, M.; Jansen, P.L. Bile acid receptors as targets for drug development. *Nat. Rev. Gastroenterol. Hepatol.* **2014**, *11*, 55–67. [[CrossRef](#)] [[PubMed](#)]
23. Lozano, E.; Monte, M.J.; Briz, O.; Hernandez-Hernandez, A.; Banales, J.M.; Marin, J.J.; Macias, R.I.R. Enhanced antitumor drug delivery to cholangiocarcinoma through the apical sodium-dependent bile acid transporter (ASBT). *J. Control. Release* **2015**, *216*, 93–102. [[CrossRef](#)] [[PubMed](#)]
24. Criado, J.J.; Herrera, M.C.; Palomero, M.F.; Medarde, M.; Rodriguez, E.; Marin, J.J. Synthesis and characterization of a new bile acid and platinum (II) complex with cytostatic activity. *J. Lipid Res.* **1997**, *38*, 1022–1032. [[CrossRef](#)] [[PubMed](#)]
25. Criado, J.J.; Macias, R.I.R.; Medarde, M.J.; Monte, M.A.; Serrano, J.J.G.; Marin, J.J. Synthesis and characterization of the new cytostatic complex cis-diammineplatinum(II) chlorocholylglycinate. *Bioconjugate Chem.* **1997**, *8*, 453–458. [[CrossRef](#)]
26. Paschke, R.; Kalbitz, J.; Paetz, C. Novel spacer linked bile acid-cisplatin compounds as a model for specific drug delivery, synthesis, and characterization. *Inorg. Chim. Acta.* **2000**, *304*, 241–249. [[CrossRef](#)]
27. Seroka, B.; Łotowski, Z.; Hryniewicka, A.; Rárová, L.; Sicinski, R.R.; Tomkiel, A.M.; Morzycki, J.W. Synthesis of new cisplatin derivatives from bile acids. *Molecules* **2020**, *25*, 655. [[CrossRef](#)] [[PubMed](#)]
28. Martinez-Diez, M.C.; Larena, M.G.; Serrano, M.A.; Macias, R.I.; Izco-Basurko, I.; Marin, J.J. Relationship between DNA-reactivity and cytostatic effect of two novel bile acid-platinum derivatives, Bamet-UD2 and Bamet-D3. *Anticancer Res.* **2000**, *20*, 3315–3321. [[PubMed](#)]
29. Criado, J.J.; Domínguez, M.F.; Medarde, M.; Fernández, E.R.; Macías, R.I.; Marín, J. Structural characterization, kinetic studies, and in vitro biological activity of new cis-diamminebis-cholylglycinate (O, O') Pt (II) and cis-diamminebis-ursodeoxycholate (O, O') Pt (II) complexes. *Bioconjugate Chem.* **2000**, *11*, 167–174. [[CrossRef](#)]
30. Briz, O.; Serrano, M.A.; Rebollo, N.; Hagenbuch, B.; Meier, P.J.; Koepsell, H.; Marin, J.J. Carriers involved in targeting the cytostatic bile acid-cisplatin derivatives cis-diammine-chloro-cholylglycinate-platinum (II) and cis-diammine-bisursodeoxycholate-platinum (II) toward liver cells. *Mol. Pharmacol.* **2002**, *61*, 853–860. [[CrossRef](#)]
31. Jiang, J.; Han, F.G.; Cai, K.X.; Shen, Q.S.; Yang, C.P.; Gao, A.L.; Yu, J.; Fan, X.M.; Hao, Y.L.; Wang, Z.; et al. Synthesis and biological evaluation of cholic acid-conjugated oxaliplatin as a new prodrug for liver cancer. *J. Inorg. Biochem.* **2023**, *243*, 112200. [[CrossRef](#)] [[PubMed](#)]

32. Kato, R.; Sato, T.; Iwamoto, A.; Yamazaki, T.; Nakashiro, S.; Yoshikai, S.; Fujimoto, A.; Imano, H.; Ijiri, Y.; Mino, Y.; et al. Interaction of platinum agents, cisplatin, carboplatin and oxaliplatin against albumin in vivo rats and in vitro study using inductively coupled plasma-mass spectrometry. *Biopharm. Drug Dispos.* **2019**, *40*, 242–249. [[CrossRef](#)] [[PubMed](#)]
33. Paschke, R.; Kalbitz, J.; Paetz, C.; Luckner, M.; Mueller, T.; Schmoll, H.J.; Mueller, H.; Sorkau, E.; Sinn, E. Cholic acid-carboplatin compounds (CarboChAPt) as models for specific drug delivery: Synthesis of novel carboplatin analogous derivatives and comparison of the cytotoxic properties with corresponding cisplatin compounds. *J. Inorg. Biochem.* **2003**, *94*, 335–342. [[CrossRef](#)] [[PubMed](#)]

Disclaimer/Publisher’s Note: The statements, opinions and data contained in all publications are solely those of the individual author(s) and contributor(s) and not of MDPI and/or the editor(s). MDPI and/or the editor(s) disclaim responsibility for any injury to people or property resulting from any ideas, methods, instructions or products referred to in the content.